both corresponding anions which are suspected to be As_6^{2-}. This formulation is not surprising since this anion would be isoelectronic (valence electrons) with Te_6^{4+}, which was recently reported as a trigonal-prismatic species.[25]

(25) R. C. Burns, R. J. Gillespie, W. C. Luk, and D. R. Slim, *Inorg. Chem.* **18**, 3086 (1979).

Acknowledgments. The author wishes to express his thanks to Dr. J. Potier for helpful discussions.

Supplementary Material Available: Tables of crypt-K^+ bond distances and angles, interionic distances, and structure factors (16 pages). Ordering information is given on any current masthead page.

Transition-Metal Complexes of Vitamin B_6 Related Compounds. 3. X-ray, Mössbauer, and Magnetic Properties of a Binuclear Iron(III) Complex Containing an Unusual Pyridoxal Derivative[1]

Gary J. Long,* James T. Wrobleski, Raju V. Thundathil, Don M. Sparlin, and Elmer O. Schlemper

Contribution from the Departments of Chemistry, University of Missouri—Rolla, Rolla, Missouri 65401, and the University of Missouri—Columbia, Columbia, Missouri 65201. *Received February 25, 1980*

Abstract: The slow air evaporation of an aqueous solution containing pyridoxal, alanine, and iron(II) perchlorate in a 2:2:1 molar ratio resulted in the precipitation of a dimeric iron(III) complex containing the previously unreported ligand $N(PL)_2ala^{2-}$ (IV). We propose that this ligand has resulted from the formation of the Schiff base between pyridoxal and pyridoxamine and the subsequent nucleophilic attack of the Schiff-base imino group upon the α-keto carbon atom of pyruvic acid. The presence of pyruvic acid and pyridoxamine is expected because of the transamination equilibrium catalyzed by the presence of iron(III). The structure of this new ligand was determined through an X-ray structural study of the resulting crystals, which were orthorhombic, *Pccn*, with $a = 13.029$ (3), $b = 20.052$ (4), $c = 19.066$ (3) Å, and $Z = 8$. The molecular structure, $\{[Fe(N(PL)_2ala)]ClO_4\}_2 \cdot 2.6H_2O$, was found to be disordered in several respects and refinement yielded a final R value of 0.087. The dimeric pseudooctahedral iron(III) structure derives from the bridging of two oxygen atoms from the α-keto groups of the two ligands present. Mössbauer and magnetic measurements indicate the presence of iron(III) ions which are antiferromagnetically coupled ($J = -5.2$ cm^{-1}) via superexchange through the two bridging oxygen atoms. The structure of this compound is similar to those of several other dimeric iron(III) compounds for which Mössbauer data are also reported. This is the first report of this ligand and the first iron(III) dimer to contain a ligand chelated to each iron ion.

Introduction

The importance of pyridoxal (I) in enzymatic transamination reactions has been known for about 50 years.[2-4] Metzler and Snell[5] and Longenecker and Snell[6] have studied the influence of various metal ions on the reversible transamination of various amino acids with pyridoxal and pyridoxamine. This work indicated that various metal ions were catalytically effective in promoting pyridoxal transamination and Metzler et al.[7] proposed a mechanism involving an amino acid–pyridoxal Schiff base intermediate which was chelated in a tridentate fashion to the metal ion.[4] The efficiency of the catalysis was found[5,6] to increase in the order $Cu^{2+} > Al^{3+} > Fe^{2+} > Fe^{3+} > Zn^{2+} > Ni^{2+} > Co^{2+}$. We have subsequently shown[2] that the studies involving divalent iron actually utilized iron(III). As a result, we have been interested in preparing and studying the iron(III) complexes containing these Shiff-base intermediates. We have recently reported[1] on several iron(III) complexes containing one tridentate Schiff-base ligand prepared from pyridoxal and glycine and are currently studying the bis complexes. Herein we report an unusual result from one of our attempted syntheses of a bis complex.

Pyridoxal can undergo a Schiff-base condensation with pyridoxamine to form the corresponding Schiff base, III.[8] Aluminum(III) and copper(II) chelates containing this ligand have been reported by Cennamo.[9] We believe, based upon the resulting solid-state structure, that, in the presence of iron(III), compound III undergoes further reaction with alanine to form the unusual dianion $N(PL)_2ala^{2-}$ (IV)[10] This is apparently the first report of this compound. Its structure was determined by single-crystal X-ray techniques in a dimeric iron(III) complex. The X-ray structure, Mössbauer, and magnetic properties of this complex are reported herein. Because of the wide interest in the bonding in oxygen-bridged systems such as $[(H_2O)_4FeOH]_2^{4-}$ we have also studied the Mössbauer-effect spectra of several related dimeric iron(III) complexes which contain the $[LFeO]_2$ bridging group.

Experimental Section

Pyridoxal hydrochloride and alanine were purchased from Sigma Chemical Co., St. Louis, Mo. Pyridoxal free base was prepared by titrating a saturated aqueous solution of the hydrochloride with 2 N KOH. Infrared spectra were recorded on a Perkin-Elmer 180 spectro-

* University of Missouri—Rolla.

(1) Part 2: Wrobleski, J. T.; Long, G. J. *Inorg. Chim. Acta* **1979**, *36*, 155.

(2) Wrobleski, J. T.; Long, G. J. *Inorg. Chem.* **1977**, *16*, 2752, and references cited therein.

(3) Holm, R. H. In "Inorganic Biochemistry", Eichhorn, G. L., Ed.; American Elsevier: New York, 1973; p 1137.

(4) Bruice, T. C.; Benkovic, S. J. "Bio-Organic Mechanism", Vol. 2; W. A. Benjamin: New York, 1966; p 181.

(5) Metzler, D. E.; Snell, E. E. *J. Am. Chem. Soc.* **1952**, *74*, 979.

(6) Longenecker, J. B.; Snell, E. E. *J. Am. Chem. Soc.* **1957**, *79*, 142.

(7) Metzler, D. E.; Ikawa, M.; Snell, E. E. *J. Am. Chem. Soc.* **1954**, *76*, 648.

(8) The systematic *Chemical Abstracts* name for this compound is 5-hydroxy-4-[[[[3-hydroxy-5-(hydroxymethyl)-2-methyl-4-pyridyl]-methylene]amino]methyl]-6-methyl-3-pyridinemethanol.

(9) Cennamo, C. *Ric. Sci.* **1968**, *38*, 31.

(10) The systematic *Chemical Abstracts* name for the protonated form of this compound, $N(PL)_2alaH_2$, is α,3-dihydroxy-β-[[[3-hydroxy-5-(hydroxymethyl)-2-methyl-4-pyridyl]methylene]amino]-5-(hydroxymethyl)-α,2-dimethyl-4-pyridinepropanoic acid.

0002-7863/80/1502-6040$01.00/0 © 1980 American Chemical Society

photometer with samples dispersed in KBr. Mössbauer-effect spectra were obtained on polycrystalline samples by using a constant acceleration Austin Science Associates Mössbauer spectrometer which was calibrated with room temperature natural α-iron foil. The $^{57}Co(Cu)$ source was maintained at room temperature for all experiments. The magnetic susceptibility measurements were obtained on a previously described[11] Faraday balance which utilized a Janis Supervaritemp helium cryostat and a Lake Shore Cryotronics temperature controller. Susceptibility measurements were obtained at eight different fields between 1000 and 8000 G and exhibited no field dependence at any temperature. All elemental analyses were performed by Galbraith Laboratories, Inc., Knoxville, Tenn.

The compound $\{[Fe(N(PL)_2ala)]ClO_4\}_2 \cdot 2.6H_2O$ was prepared by mixing iron(II) perchlorate, free base pyridoxal, and alanine in a 1:2:2 molar ratio in water. No attempt was made to exclude oxygen from the system. Upon mixing, the solution immediately turned to a very dark red color. No immediate precipitate occurred. Over a period of a few weeks, slow evaporation at room temperature yielded deep red to black, approximately diamond shaped crystals. Because of the deep color of the crystals it has not been possible to measure any optical extinctions. Several well-formed crystals were selected for crystallography and the remaining bulk of the material was used for subsequent magnetic, infrared, and analytical work. The empirical formula for the asymmetric unit, as derived from the X-ray structure (see below), is $Fe(N(PL)_2ala)ClO_4 \cdot 1.3H_2O$, $Fe(C_{19}H_{21}N_3O_7)ClO_4 \cdot 1.3H_2O$, or $FeC_{19}H_{23.6}N_3O_{12.3}Cl$. Elemental analysis gave the following results: Fe, 8.90; C, 36.09; H, 4.18; N, 6.91; O, 38.31 (by difference); Cl, 5.61. These experimental results correspond to the empirical formula $FeC_{19}H_{26}N_3O_{15}Cl$. The 15 oxygen atoms indicate that the bulk material could contain up to four water molecules per asymmetric unit. This would correspond to $Fe(C_{19}H_{21}N_3O_7)ClO_4 \cdot 4H_2O$ or $FeC_{19}H_{29}N_3O_{15}Cl$ and calculated values of Fe, 8.85; C, 36.18; H, 4.63; N, 6.66 O, 38.05; Cl, 5.62. With the exception of hydrogen, these calculated values are in excellent agreement with the experimental results. The difference in the number of waters of hydration between the bulk material and the single crystal studied can be accounted for in two ways. Either the bulk material may have variable amounts of water with an average of four, or the well-formed crystals may contain less water than the bulk material.

X-ray Diffraction Data Collection and Reduction. Preliminary film results and diffractometer measurements indicated that the crystals were orthorhombic (*Pccn*, with $a = 13.029$ (3), $b = 20.052$ (4), and $c = 19.066$ (3) Å). This corresponds to a unit cell volume of 4981 Å^3 and with $Z = 8$ (or four dimers per unit cell) the calculated density is 1.55 g/cm^3. The observed density, determined by flotation in a CCl_4–cyclohexane solution, is 1.57 (2) g/cm^3. The systematic extinctions were odd l on $0kl$ and $h0l$ and odd $h + k$ on $hk0$. The cell dimensions were obtained by a least-squares fit on the setting angle for 15 manually centered reflections on a Picker four-angle programmed diffractometer. The intensities of three standard reflections were measured after every 50 reflections, and the data were corrected for an approximately 5% overall decrease in intensity. The data were collected (by using Mo Kα radiation of 0.7107-Å wavelength) up to a maximum 2θ value of 40°. Additional details covering data collection are described elsewhere.[11] The integrated and Lorentz-polarization corrected data were then corrected for absorption ($\mu = 12.4$ cm^{-1}, transmission range = 0.58–0.67, and crystal dimensions of approximately 0.2 × 0.4 × 0.6 mm) by an analytical method.[12] The data were then sorted and averaged to yield 3252 independent reflections (agreement factor = 0.040) of which the 2390 reflections with $F_o^2 > 2\sigma(F_o^2)$ were used in the subsequent refinement of the structure. The 2σ value was calculated from the expression $\sigma(F_o^2)^2 = \sigma_{count}^2 + (0.05F_o^2)^2$, where σ is the estimated error in the value of F_o^2.

X-ray Structure Solution and Refinement. The structure was solved by conventional Patterson and Fourier methods. The solution was somewhat difficult because of the disorder and partial occupancy problems encountered. Partial occupancy factors were refined for two oxygen positions for each hydroxymethyl group, and the sum of these values was within experimental error of unity in each case. These two positions are likely to be coupled with the partical occupancy of the water positions because of hydrogen bonding (see below for details). In the final solution, both hydroxymethyl oxygen atoms are disordered, and the 1.3 water molecules in the asymmetric unit are in two partially occupied sites. The perchlorate oxygen atoms are not well resolved, but the final model has them in ordered, fully occupied, highly thermally smeared positions. These complications are reflected in the final agreement factors: $R = \sum||F_o| - k|F_c||/\sum F_o = 0.087$ and $wR = (\sum w(|F_o| - k|F_c|)^2/\sum wF_o^2)^{1/2} = 0.108$, where $w = 1/\sigma(F_o)$ and $\sigma(F_o) = \sigma(F_o^2)/2.0*F_o$. The final full-matrix least-squares refinement cycle had 352 variables which included anisotropic thermal parameters and positional parameters for all 39 independent nonhydrogen atoms and one overall scale factor. The partial occupancy factors were fixed at values from previous cycles of refinement. Anomalous scattering factors[13] were included in F_c[14] for the iron and chlorine atoms, and the atomic scattering factors were taken from the work of Cromer and Waber.[15] A final difference Fourier synthesis revealed no electron density greater than 0.8 e/Å^3.

The observed and calculated structure factors are available elsewhere.[16] The final positional and thermal parameters are presented in Table I.[17]

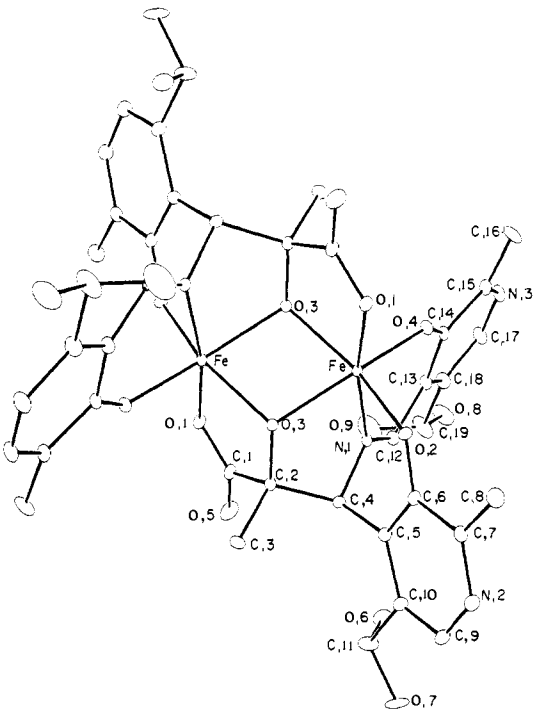

Figure 1. ORTEP drawing and numbering scheme for $[Fe(N(PL)_2ala]_2$ X-ray structure.

Results and Discussion

The iron complex under study is stable and no apparent decomposition of the crystals was observed even after long storage in a closed container. The crystals do, however, slowly degrade in the X-ray beam. Qualitative analysis indicated the absence of any chloride or alkali-metal ions in the compound.

The infrared spectrum of $\{[Fe(N(PL)_2ala)]ClO_4\}_2 \cdot 2.6H_2O$ is rather complex and its interpretation is made more difficult because no comparison can be made with the free ligand spectrum. The presence of ionic perchlorate is clearly indicated by three strong bands at 1085, 1110, and 1190 cm^{-1}. Lattice water is indicatd by a strong, broad band centered at 3360 cm^{-1}. Some tentative assignments for ligand-associated bands are possible through a comparison with other pyridoxal–amino acid Schiff-base metal complexes.[2] Hence we assign a strong band at 1625 cm^{-1} to $\nu_{C=N}$, a strong doublet at 1495 and 1515 cm^{-1} to the phenolic ν_{CO} stretch, a strong band at 1587 cm^{-1} to an asymmetric carboxyl stretch, and a strong broad band at 1360 cm^{-1} to the symmetric carboxyl stretching mode. This accounts for all the strong infrared

(11) Long, G. J.; Longworth, G.; Battle, P.; Cheetham, A. K.; Thundathil, R. V.; Beveridge, D. *Inorg. Chem.* **1979**, *18*, 624. Long, G. J.; Schlemper, E. O. *Ibid.* **1974**, *13*, 279.

(12) All calculations were performed on the IBM 370/168 computer of the University of Missouri–Columbia Computer Research Center, with the following programs: W. C. Hamilton, SORTH, sorting program; ANGSET, angle setting program; W. C. Hamilton, HORSE, general absorption program; R. Doedens and J. A. Ibers, NUCLS, least-squares program, a modification of W. Busing and H. Levy's program; A. Zalkin, FORDAP, Fourier program; W. Busing and H. Levy, ORFFE, function and error program; C. Johnson, ORTEP, thermal ellipsoid plot program; local data processing programs.

(13) Cromer, D. T. *Acta Crystallogr.* **1962**, *18*, 17.

(14) Ibers, J. A.; Hamilton, W. C. *Acta Crystallogr.* **1964**, *19*, 781.

(15) Cromer, D. T.; Waber, J. T. *Acta Crystallogr.* **1962**, *18*, 104.

(16) The structure factor table will appear in the microfilm edition of this journal. See paragraph at end of paper regarding supplementary material.

(17) Numbers in parentheses here and elsewhere in this paper indicate estimated standard deviations in the least significant digits.

Table I. Final Positional and Anisotropic Thermal ($\times 10^4$) Parameters for Nonhydrogen Atoms[a]

atom	x	y	z	β_{11}	β_{22}	β_{33}	β_{12}	β_{13}	β_{23}
Fe	0.0158 (1)	0.0314 (1)	0.0758 (1)	53 (1)	21(1)	19 (1)	−0 (1)	−0 (1)	−2 (1)
Cl	−0.1917 (5)	0.1809 (4)	−0.3056 (3)	177 (6)	103 (3)	70 (2)	−26 (3)	19 (3)	−18 (2)
O(1)	0.1338 (4)	−0.0276 (3)	0.1030 (3)	60 (4)	27 (2)	30 (2)	5 (2)	−9 (2)	−6 (2)
O(2)	0.1083 (5)	0.1037 (3)	0.0980 (3)	71 (5)	21 (2)	34 (2)	−5 (2)	−7 (3)	−1 (2)
O(3)	−0.0243 (5)	−0.0540 (3)	0.0280 (3)	77 (5)	21 (2)	21 (2)	4 (2)	5 (2)	−1 (1)
O(4)	−0.0527 (5)	0.0144 (3)	0.1651 (3)	62 (5)	34 (2)	23 (2)	3 (2)	6 (2)	2 (2)
O(5)	0.1931 (7)	−0.1294 (4)	0.1072 (5)	125 (7)	42 (3)	73 (4)	33 (4)	−49 (5)	−15 (3)
O(6)	−0.1642 (12)	0.2900 (6)	0.0159 (8)	124 (13)	37 (4)	65 (6)	9 (6)	−18 (7)	1 (4)
O(7)	−0.0488 (19)	0.3673 (9)	−0.0015 (14)	163 (24)	16 (6)	100 (13)	−8 (9)	−27 (15)	18 (7)
O(8)	−0.4899 (7)	0.1204 (7)	0.1761 (7)	57 (8)	103 (7)	71 (6)	25 (6)	16 (5)	31 (5)
O(9)	−0.3943 (33)	0.1047 (34)	0.0809 (29)	104 (33)	163 (36)	92 (25)	−10 (28)	−34 (26)	41 (27)
O(10)	0.0394 (14)	0.2317 (8)	0.2495 (9)	139 (16)	65 (7)	59 (7)	42 (9)	6 (9)	−10 (6)
O(11)	0.2811 (16)	0.0453 (10)	−0.0180 (10)	274 (24)	137 (11)	116 (10)	−83 (13)	70 (13)	−26 (8)
O(12)	−0.2789 (14)	0.1835 (10)	−0.2620 (8)	258 (20)	193 (13)	85 (7)	−20 (13)	51 (10)	−32 (8)
O(13)	−0.1983 (22)	0.2347 (8)	−0.3438 (12)	593 (49)	89 (7)	178 (15)	52 (15)	174 (22)	72 (9)
O(14)	−0.1957 (19)	0.1315 (11)	−0.3505 (10)	483 (36)	148 (12)	117 (10)	110 (16)	−6 (15)	−60 (9)
O(15)	−0.1058 (16)	0.1783 (15)	−0.2699 (18)	223 (21)	251 (20)	332 (27)	22 (16)	−177 (21)	−124 (20)
N(1)	−0.0968 (5)	0.1045 (3)	0.0642 (3)	62 (6)	23 (2)	20 (2)	−1 (3)	2 (3)	−3 (2)
N(2)	0.1709 (8)	0.2749 (5)	0.1016 (5)	118 (9)	35 (3)	39 (3)	−23 (4)	−3 (5)	−3 (3)
N(3)	−0.2734 (7)	0.0078 (5)	0.2720 (4)	87 (8)	54 (4)	23 (3)	−11 (4)	7 (4)	1 (2)
C(1)	0.1272 (8)	−0.0887 (6)	0.0896 (5)	81 (8)	33 (4)	29 (3)	9 (5)	−4 (4)	−8 (3)
C(2)	0.0293 (7)	−0.1112 (4)	0.0513 (5)	71 (7)	26 (3)	22 (3)	5 (4)	0 (4)	−2 (2)
C(3)	−0.0378 (9)	−0.1520 (5)	0.1039 (5)	121 (10)	31 (3)	31 (3)	−9 (5)	20 (5)	8 (3)
C(4)	−0.0636 (7)	0.1533 (4)	0.0121 (5)	78 (7)	20 (3)	29 (3)	−5 (4)	8 (4)	−1 (2)
C(5)	0.0181 (8)	0.1955 (5)	0.0453 (5)	81 (8)	25 (3)	30 (3)	−1 (4)	−2 (5)	−1 (3)
C(6)	0.0976 (8)	0.1664 (5)	0.0848 (5)	77 (8)	29 (3)	28 (3)	−16 (4)	10 (4)	−6 (3)
C(7)	0.1777 (8)	0.2091 (6)	0.1136 (5)	95 (9)	38 (4)	26 (3)	−22 (5)	2 (5)	−0 (3)
C(8)	0.2663 (9)	0.1820 (6)	0.1533 (6)	90 (9)	52 (4)	45 (5)	−19 (5)	−19 (6)	0 (4)
C(9)	0.0946 (11)	0.3037 (5)	0.0646 (6)	134 (12)	30 (3)	41 (5)	−26 (6)	−4 (6)	−5 (3)
C(10)	0.0182 (9)	0.2662 (5)	0.0363 (6)	125 (11)	25 (3)	38 (4)	−12 (5)	12 (6)	−2 (3)
C(11)	−0.0638 (11)	0.3010 (6)	−0.0092 (7)	95 (10)	32 (4)	67 (6)	11 (5)	−2 (6)	17 (4)
C(12)	−0.1831 (8)	0.1145 (5)	0.0955 (5)	70 (8)	36 (3)	28 (3)	−1 (4)	3 (4)	1 (3)
C(13)	−0.2163 (7)	0.0711 (5)	0.1537 (5)	53 (7)	37 (3)	26 (3)	2 (4)	4 (4)	−1 (3)
C(14)	−0.1456 (8)	0.0266 (5)	0.1869 (4)	74 (8)	32 (3)	19 (3)	−15 (4)	1 (4)	−2 (2)
C(15)	−0.1747 (8)	−0.0035 (5)	0.2508 (5)	72 (9)	39 (3)	25 (3)	−12 (4)	11 (4)	−4 (3)
C(16)	−0.1068 (9)	−0.0458 (6)	0.2931 (6)	94 (9)	63 (5)	34 (4)	17 (5)	0 (5)	24 (4)
C(17)	−0.3435 (8)	0.0455 (6)	0.2401 (6)	70 (8)	59 (5)	31 (4)	5 (5)	3 (5)	7 (3)
C(18)	−0.3155 (8)	0.0778 (6)	0.1794 (6)	66 (8)	50 (4)	37 (4)	−3 (5)	12 (5)	2 (3)
C(19)	−0.3946 (10)	0.1221 (10)	0.1423 (9)	65 (10)	112 (9)	53 (6)	41 (8)	16 (7)	29 (7)

[a] The anisotropic temperature factors ($\times 10^4$) are of the form $\exp[-(\beta_{11}h^2 + \beta_{22}k^2 + \beta_{33}l^2 + 2\beta_{12}hk + 2\beta_{13}hl + 2\beta_{23}kl)]$.

bands except for one at 620 cm^{-1} which we tentatively assign to ν_{Fe-O}.

X-ray Structure. The structure of the dimeric iron-containing portion of $\{[Fe(N(PL)_2ala)]ClO_4\}_2 \cdot 2.6H_2O$ is presented in Figure 1 along with the atom numbering scheme. Intramolecular bond distances are presented in Table II[18] and bond angles in Table III.[18] This dimer is apparently the first to contain a ligand which is coordinated to both iron(III) ions by atoms other than the bridging oxygen atom. Several other iron(III) dimers have been reported[19-23] which have very similar bridging coordination geometry but do not have ligands which chelate both metals. The bridging coordination geometry of these related iron(III) dimers is compared with that of the compound under study in Table IV.

The iron(III) ion coordination geometry is highly distorted from octahedral geometry with angles ranging from 76.2 to 111.6°. The distortions are, however, what one might expect from the chelation geometry of the ligand. The four-membered bridging ring has the smallest angle (76.2°). The two five-membered chelation rings have smaller (77.2° for O(3)'-Fe-N(1) and 79.3° for O(3)-Fe-O(1)) bonding angles than the two six-membered chelation rings (with 86.2° for O(2)-Fe-N(1) and 93.2° for O(4)-Fe-N(1)). The overall average of the four chelation angles is 84.0°, whereas the average of the seven nonchelated octahedral angles is 98.4°. Hence the distortion from octahedral geometry appears to result from the bonding constraints of the ligand. This octahedral distortion is also exhibited in the atom deviations from the best plane[24] through the Fe, O(2), O(3), O(3)', and O(4) atoms. The Fe is only 0.02 Å above this plane while O(2) and O(3) are

Table II. Intramolecular Bond Distances (Å)

Fe-Fe'	3.180(3)	N(1)-C(12)	1.29(1)
Fe-O(1)	2.008(6)	N(2)-C(7)	1.34(1)
Fe-O(2)	1.933(6)	N(2)-C(9)	1.35(1)
Fe-O(3)	2.008(5)	N(3)-C(15)	1.37(1)
Fe-O(3)'	2.033(5)	N(3)-C(17)	1.33(1)
Fe-O(4)	1.953(6)	C(1)-C(2)	1.54(1)
Fe-N(1)	2.087(7)	C(2)-C(3)	1.56(1)
Cl-O(12)	1.41(1)	C(2)'-C(4)	1.54(1)
Cl-O(13)	1.31(1)	C(4)-C(5)	1.50(1)
Cl-O(14)	1.31(1)	C(5)-C(6)	1.41(1)
Cl-O(15)	1.31(1)	C(5)-C(10)	1.43(1)
O(1)-C(1)	1.25(1)	C(6)-C(7)	1.46(1)
O(2)-C(6)	1.29(1)	C(7)-C(8)	1.48(2)
O(3)-O(3)'	2.49(1)	C(9)-C(10)	1.36(1)
O(3)-C(2)	1.42(1)	C(10)-C(11)	1.54(2)
O(4)-C(14)	1.30(1)	C(12)-C(13)	1.48(1)
O(5)-C(1)	1.23(1)	C(13)-C(14)	1.43(1)
O(6)-C(11)	1.41(2)	C(13)-C(18)	1.39(1)
O(7)-C(11)	1.35(2)	C(14)-C(15)	1.41(1)
O(8)-C(19)	1.40(2)	C(15)-C(16)	1.47(1)
O(9)-C(19)	1.22(5)	C(17)-C(18)	1.38(1)
N(1)-C(4)	1.46(1)	C(18)-C(19)	1.53(2)

(18) Unprimed atoms are located at x, y, z, and primed atoms are located at $-x, -y, -z$.

(19) Thich, J. A.; Ou, C. C.; Powers, D.; Vasiliou, B.; Mastropaolo, D.; Potenza, J. A.; Schugar, H. J. *J. Am. Chem. Soc.* **1976**, *98*, 1425.

(20) Ou, C. C.; Lalancette, R. A.; Potenza, J. A.; Schugar, H. J. *J. Am. Chem. Soc.* **1978**, *100*, 2053.

(21) Bertrand, J. A.; Eller, P. G. *Inorg. Chem.* **1974**, *13*, 927.

(22) Bertrand, J. A.; Breece, J. L.; Eller, P. G. *Inorg. Chem.* **1974**, *13*, 125.

(23) Bertrand, J. A.; Breece, J. L.; Kalyanaraman, A. R.; Long, G. J.; Baker, Jr., W. A. *J. Am. Chem. Soc.* **1970**, *92*, 5233.

(24) The equation for the best mean plane through atoms Fe, O(2), O(3), O(3)', and O(4) is $-0.8345x + 0.5333y - 0.1383z = 0.01417$.

Table III. Bond Angles (deg)

O(1)-Fe-O(2)	84.7(3)	C(1)-C(2)-C(4)'	107.0(7)
O(1)-Fe-O(3)	79.3(2)	C(3)-C(2)-C(4)'	112.2(7)
O(1)-Fe-O(3)'	109.9(2)	N(1)-C(4)-C(2)'	104.6(7)
O(1)-Fe-O(4)	91.2(2)	N(1)-C(4)-C(5)	107.5(7)
O(1)-Fe-N(1)	168.5(2)	C(2)'-C(4)-C(5)	115.7(8)
O(2)-Fe-O(3)	90.7(2)	C(4)-C(5)-C(6)	121.0(8)
O(2)-Fe-O(3)	154.3(3)	C(4)-C(5)-C(10)	120.6(9)
O(2)-Fe-O(4)	103.0(3)	C(6)-C(5)-C(10)	118.4(9)
O(2)-Fe-N(1)	86.2(3)	O(2)-C(6)-C(5)	126.0(8)
O(3)-Fe-O(3)'	76.2(2)	O(2)-C(6)-C(7)	115(1)
O(3)-Fe-O(4)	97.4(2)	C(5)-C(6)-C(7)	119.0(9)
O(3)'-Fe-O(4)	155.9(3)	N(2)-C(7)-C(6)	117(1)
O(3)'-Fe-N(1)	77.2(2)	N(2)-C(7)-C(8)	119.8(9)
O(3)-Fe-N(1)	111.6(2)	C(6)-C(7)-C(8)	122(1)
O(4)-Fe-N(1)	93.2(3)	N(2)-C(9)-C(10)	121(1)
O(12)-Cl-O(13)	104(1)	C(5)-C(10)-C(9)	120(1)
O(12)-Cl-O(14)	112(1)	C(5)-C(10)-C(11)	121(1)
O(12)-Cl-O(15)	112(2)	C(9)-C(10)-C(11)	119(1)
O(13)-Cl-O(14)	105(2)	O(6)-C(11)-O(7)	104(2)
O(13)-Cl-O(15)	112(2)	O(6)-C(11)-C(10)	112(1)
O(14)-Cl-O(15)	110(2)	O(7)-C(11)-C(10)	107(1)
Fe-O(1)-C(1)	118.0(6)	N(1)-C(12)-C(13)	120.9(9)
Fe-O(2)-C(6)	128.4(6)	C(12)-C(13)-C(14)	120.8(8)
Fe-O(3)-Fe'	103.8(2)	C(12)-C(13)-C(18)	118.8(9)
Fe-O(3)-C(2)	114.8(5)	C(14)-C(13)-C(18)	120.2(9)
Fe'-O(3)-C(2)	117.4(5)	O(4)-C(14)-C(13)	125.1(8)
Fe-O(4)-C(14)	132.0(6)	O(4)-C(14)-C(15)	116.3(9)
Fe-N(1)-C(4)	109.5(4)	C(13)-C(14)-C(15)	118.4(9)
Fe-N(1)-C(12)	132.3(6)	N(3)-C(15)-C(14)	116(1)
C(4)-N(1)-C(12)	118.0(8)	N(3)-C(15)-C(16)	120.0(9)
C(7)-N(2)-C(9)	123.9(9)	C(14)-C(15)-C(16)	124(1)
C(15)-N(3)-C(17)	127.2(9)	N(3)-C(17)-C(18)	118(1)
O(1)-C(1)-O(5)	123.0(9)	C(13)-C(18)-C(17)	120(1)
O(1)-C(1)-C(2)	116.1(9)	C(13)-C(18)-C(19)	121(1)
O(5)-C(1)-C(2)	120.9(9)	C(17)-C(18)-C(19)	119(1)
O(3)-C(2)-C(1)	108.7(7)	O(8)-C(19)-O(9)	116(3)
O(3)-C(2)-C(3)	110.5(7)	O(8)-C(19)-C(18)	112(1)
O(3)-C(2)-C(4)'	110.0(7)	O(9)-C(19)-C(18)	106(3)
C(1)-C(2)-C(3)	108.3(8)		

0.31 and 0.37 Å above this plane and O(4) and O(3)′ are 0.30 and 0.40 Å below this plane.

In constrast to the other dimeric structures listed in Table IV, the Fe–O(3) and Fe–O(3)′ bond distances in $\{[Fe(N(PL)_2ala)]ClO_4\}_2 \cdot 2.6H_2O$ are only marginally different (0.025 Å or 2.5σ) but are significantly longer than those reported for the dihydroxy-[19,20] and alkoxy-bridged[21-23] dimers. These longer bonding distances are also reflected in the somewhat longer Fe–Fe′ (3.180 Å) and O(3)–O(3)′ (2.49 Å) distances as compared with the dihydroxy-bridged dimers. In all of these complexes the nonbonded bridging-oxygen to bridging-oxygen distance is significantly less than the ca. 3.0 Å sum for their van der Waals radii.[25] It is, however, similar to the ca. 2.4 Å sum for the oxide effective ionic radius.[26] The relatively long O(3)–O(3)′ distance may result from constraints arising from the unique bridging nature of this ligand.

In general the remaining bond distances and angles for the bridge and for the ligand itself are reasonable. The short 1.29 (1) Å N(1)–C(12) bond distance indicates the expected presence of a double bond. An examination of about 50 structures published during the past year indicates a range of 1.28–1.31 Å for nondelocalized carbon to nitrogen double bonds. Both of the hydroxymethyl groups contained in the pyridoxal moiety show extensive disorder but rather small vibrational anisotropy. For the first of these groups, O(6) and O(7) show an average occupancy of 0.625 and 0.375. For the second, O(8) and O(9) show an average occupancy of 0.73 and O.27.

The Mössbauer and magnetic properties (see below) clearly indicate that the iron in this complex is trivalent. Hence, in order to obtain charge balance for the complex, each ligand must be a dianion. As a result, we have formulated the ligand as shown in IV as the dizwitterionic dianion in which the two phenoxy-oxygen anionic charges are compensated by protonation of the two pyridoxal heterocyclic nitrogen atoms. This formulation is consistent with the preparation. Unfortunately these hydrogen ions could not be located in the crystallographic work. Their presence is indicated by potential hydrogen bonding between N(3) and O(1), N(2) and O(5), and N(2) and O(12). These and additional hydrogen bonds and their distances are listed in Table V. The additional positive charge on the iron ion is balanced by the presence of a perchlorate ion. The perchlorate oxygen atoms are fully occupied but highly thermally smeared. They also participate in several hydrogen bonds with both the ligand and the lattice water. The 1.3 lattice water molecules found in the asymmetric unit are in two partially occupied sites and have refined occupancy factors of 0.52 for O(10) and 0.81 for O(11).

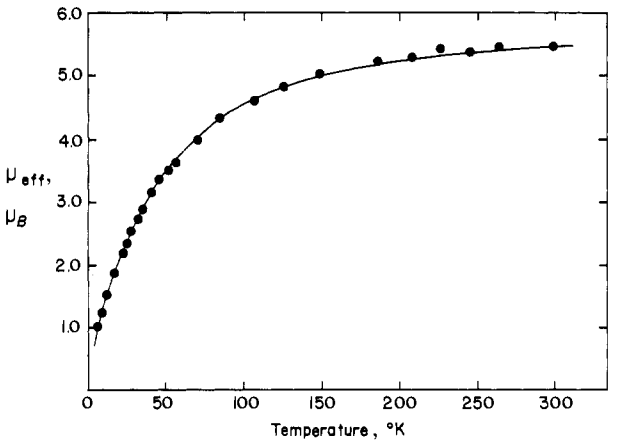

Figure 2. A plot of the magnetic moment of $\{[Fe(N(PL)_2ala)]ClO_4\}_2 \cdot 2.6H_2O$ as a function of temperature. The solid line corresponds to a calculated fit for $S = {}^5/_2$, $g = 2.00$, and $J = -5.2$ cm^{-1} (see text).

Magnetic Properties. The magnetic properties of $\{[Fe(N(PL)_2ala)]ClO_4\}_2 \cdot 2.6H_2O$ have been studied from room temperature to 4.8 K. The results are presented in Table VI and shown in Figure 2. As might be expected for a binuclear bridged iron(III) dimer, this complex exhibits weak antiferromagnetic coupling between the iron ions with a maximum in the susceptibility (the Néel temperature) at ca. 50 K. We have used the Heisenberg–Dirac–Van Vleck model[27] to evaluate the magnitude of the spin–spin superexchange coupling between the two iron(III) ions. The best fit, which assumed $S_1 = S_2 = {}^5/_2$ and $g = 2.00$, was in essentially perfect agreement with the experimental data for an antiferromagnetic exchange coupling constant, J, of −5.2 (2) cm^{-1}. The calculated values are shown as the solid line in Figure 2.

There has long been interest in the geometry of the bridging superexchange pathway and the magnitude and sign (ferromagnetic or antiferromagnetic) of the magnetic spin–spin exchange coupling.[28,29] Hatfield and his co-workers have been successful in establishing such a relationship in an extensive series of dioxygen bridged copper dimers. The most important factor in determining the exchange properties in these complexes appears to be the angle at the bridging oxygen atoms. Hence, it is interesting to compare the magnetic coupling in $\{[Fe(N(PL)_2ala)]ClO_4\}_2 \cdot 2.6H_2O$ with that found in other iron(III) dimers. There have been many reports of the magnetic properties of oxo-bridged iron(III) dimers,[30,31] but relatively few reports of structures containing two oxygen atoms bridging iron(III) ions. In fact, complete structural work has been reported for only five other such complexes.[19-22]

(25) Bondi, A. *J. Phys. Chem.* **1964**, *68*, 441.
(26) Shannon, R. D. *Acta Crystallogr., Sect. A* **1976**, *32*, 751.
(27) Martin, R. L. In "New Pathways in Inorganic Chemistry", Ebsworth, E. A. V., Maddock, A. G., Sharpe, A. G., Eds.; Cambridge University Press: New York, 1968; p 175.
(28) Ginsberg, A. P. *Inorg. Chim. Acta* **1971**, *5*, 45.
(29) Crawford, V. H.; Richardson, H. W.; Wasson, J. R.; Hodgson, D. J.; Hatfield, W. E. *Inorg. Chem.* **1976**, *15*, 2107.
(30) Reiff, W. M.; Long, G. J.; Baker, Jr., W. A. *J. Am. Chem. Soc.* **1968**, *90*, 6347, and references cited therein.
(31) Murray, K. S. *Coord. Chem. Rev.* **1974**, *12*, 1.

Table IV. Structural Properties of Several Related Iron(III) Dimers[a]

compd	Fe-Fe'	O-O'	Fe-O	Fe-O-Fe'	O-Fe-O'	$-J$, cm^{-1}	ref
$[Fe(N(PL)_2ala)ClO_4]_2 \cdot 2.6H_2O$	3.180(3)	2.49(1)	2.008(5) 2.033(5)	103.8(2)	76.2(2)	5.2	this work
$[Dipic(H_2O)FeOH]_2$	3.089(2)	2.431	1.938(5) 1.993(5)	103.6(2)	76.4(2)	11.4	19
$[Chel(H_2O)FeOH]_2 \cdot 4H_2O$	3.078(2)	2.438	1.938(4) 1.989(4)	103.2(2)	76.8(2)	7.3	19
$[Me_2Npic(H_2O)FeOH]_2 \cdot 2H_2O$	3.118(3)	2.381	1.937(6) 1.986(9)	105.3(4)	74.7(4)	11.7	20
$[Fe(Salpa)(Salpah)]_2 \cdot$toluene	3.217(7)	2.28(3)	1.97(2) 1.92(2)	110.6(9)	70.2(8)	17	21
			1.93(2) 2.00(2)	108.2(9)	70.9(8)		
$[Fe(Salpa)Cl]_2 \cdot$toluene	3.089(6)	2.393	1.93(1) 1.98(1)	104.1(6)	75.9(6)	17	22
$[Fe(Salpa)Cl]_2$	3.12	2.23	1.97 1.86	109.0	71.0	17	23

[a] Bond distances in angstroms, angles in degrees. Abbreviations: Dipic, 2,6-pyridinedicarboxylate; Chel, 4-hydroxo-2,6-pyridinedicarboxylate; Me_2Npic, 4-(dimethylamino)-2,6-pyridinedicarboxylate; Salpa, 3-hydroxypropylsalicylaldimine; Salpah, protonated monoanion of Salpa.

Table V. Potential Hydrogen-Bond Distances (Å)

O(1)-O(11)	3.34	O(6)-N(2)	3.37
O(1)-N(3)	2.77	O(7)-O(9)	2.59
O(2)-O(11)	3.37	O(7)-O(11)	2.85
O(3)-O(11)	3.36	O(8)-O(10)	2.67
O(5)-N(2)	2.61	O(10)-O(12)	2.92
O(6)-O(11)	3.38	O(10)-O(14)	2.64
O(6)-O(13)	2.76	O(11)-O(15)	3.06
O(6)-O(15)	3.02	O(12)-N(2)	3.24

Table VI. Magnetic Susceptibility Results

T, K	$\chi'_M \times 10^6$, cgsu	$\chi'_{Fe} \times 10^6$, cgsu	$1/\chi'_{Fe}$, cgsu^{-1}	μ_{eff}, μ_B
296.5	25 420	12 710	78.7	5.49
288.0	26 940	13 470	74.2	5.57
262.5	29 560	14 780	67.7	5.47
244.5	30 490	15 250	65.6	5.46
225.5	32 940	16 470	60.7	5.45
207.0	33 680	16 840	59.4	5.28
185.5	37 300	18 650	53.6	5.26
167.0	40 490	20 250	49.4	5.20
147.5	43 410	21 710	46.1	5.06
125.0	47 450	23 720	42.2	4.87
105.5	51 470	25 740	38.9	4.66
82.0	57 970	28 990	34.5	4.36
69.4	59 100	29 550	33.8	4.05
56.3	59 830	29 910	33.4	3.67
51.2	61 210	30 600	32.7	3.54
46.0	60 650	30 320	33.0	3.34
40.7	60 970	30 480	32.8	3.15
34.1	59 990	29 990	33.3	2.86
31.1	59 490	29 750	33.6	2.72
27.2	58 850	29 430	34.0	2.53
24.4	57 080	28 540	35.0	2.36
21.0	56 070	28 040	35.7	2.17
15.6	53 680	26 840	37.2	1.83
10.9	53 010	26 500	37.7	1.52
7.63	52 030	26 020	38.4	1.26
4.80	55 270	27 640	36.2	1.03

A comparison of the magnetic exchange coupling constant with the bridging structure (Table IV) reveals rather little correlation with geometry. As was concluded earlier,[19] there seems to be little evidence for direct iron–iron bonding to account for the magnitude of antiferromagnetic exchange. Both the complex under study herein and $[Fe(Salpa)(Salpah)]_2$ have the longest Fe–Fe' bond distances and the most widely differing J values (i.e., -5.2 and -17 cm^{-1}). In general, there seems to be little correlation between the magnitude of the exchange and the Fe–O–Fe' bridging angle. It should be noted, however, that $\{[Fe(N(PL)_2ala)]ClO_4\}_2 \cdot 2.6H_2O$, which has the weakest exchange coupling observed to date in this type of complex, also has the longest Fe–O–Fe superexchange distance. The average Fe–O bridging bond distance is 2.02 Å for this compound as compared with an average of 1.96 Å for the remaining Fe–O distances listed in Table IV. Hence there may be some evidence for a decrease in magnetic spin–spin exchange coupling with increasing superexchange distance. Alternatively, it is interesting to note that $\{[Fe(N(PL)_2ala)]ClO_4\} \cdot 2.6H_2O$ does not contain any direct intermolecular hydrogen bonding. This lack of intermolecular hydrogen bonded exchange pathways may account for the weaker antiferromagnetic coupling in this compound as compared with the dihydroxo-bridged dimers in which such pathways are certainly present. Additional data, including magnetic studies to temperatures below 78 K in order to improve the accuracy of the exchange coupling constants,[21,22] will be required to definitely establish these correlations.

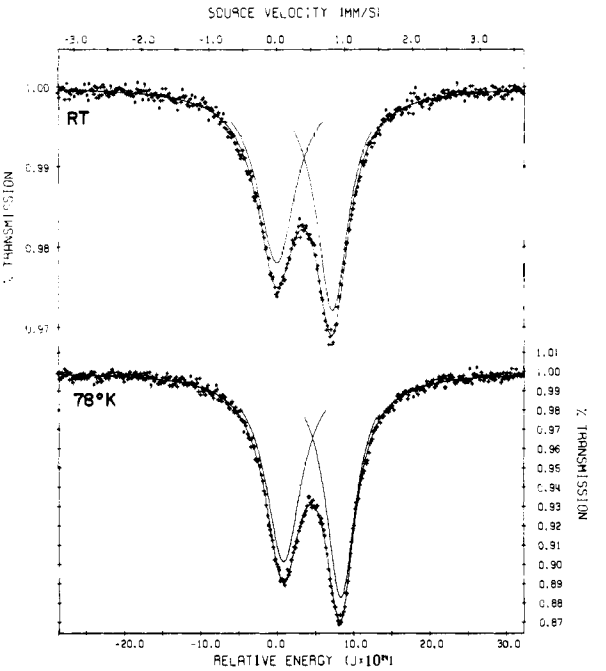

Figure 3. The Mössbauer effect spectrum of $\{[Fe(N(PL)_2ala)]ClO_4\}_2 \cdot 2.6H_2O$ obtained at room temperature and 78 K.

Mössbauer Spectral Properties. The Mössbauer effect spectrum of $\{[Fe(N(PL)_2ala)]ClO_4\}_2 \cdot 2.6H_2O$ has been measured at room temperature and 78 K and the results are shown in Figure 3. Because of the interest in oxygen-bridged compounds as possible models for the $[(H_2O)_4FeOH]_2^{4+}$ species,[19] we have also measured the Mössbauer spectra of several of the related oxygen-bridged compounds.[32] Mössbauer spectral parameters for all these

(32) We wish to thank Dr. J. A. Bertrand of the Georgia Institute of Technology for providing us with these compounds.

Table VII. Mössbauer Effect Spectral Data[a]

compd	T, K	ΔE_Q	δ	Γ_1	Γ_2	$A_{2/1}$	$I_{2/1}$
$[Fe(N(PL)_2ala)ClO_4]_2 \cdot 2.6H_2O$	78	0.83	0.51	0.62	0.53	1.01	1.19
	RT	0.80	0.41	0.66	0.56	1.08	1.27
$[Fe(Salpa)(Salpah)]_2 \cdot$toluene	78	0.68	0.51	0.31	0.34	0.96	0.87
	RT	0.72	0.40	0.46	0.47	0.92	0.89
$[Fe(Salpa)Cl]_2 \cdot$toluene	78	1.03	0.43	0.30	0.31	0.97	0.92
	RT	1.02	0.33	0.29	0.33	0.85	0.75
$[Fe(Salpa)Cl]_2$[b]	78	1.03	0.44	0.27	0.26	1.03	1.04
	RT	1.00	0.33	0.31	0.26	1.13	1.34
$Fe(Sane)_2Cl$	78	1.36	0.52	0.31	0.33	1.00	0.92
	RT	1.60	0.34	0.31	0.37	1.01	0.83

[a] All data in mm/s relative to natural α-iron foil. Abbreviations are as given in Table IV and Sane is *N*-2-phenylethylsalicylaldimine. [b] Data taken from ref 23.

Scheme I

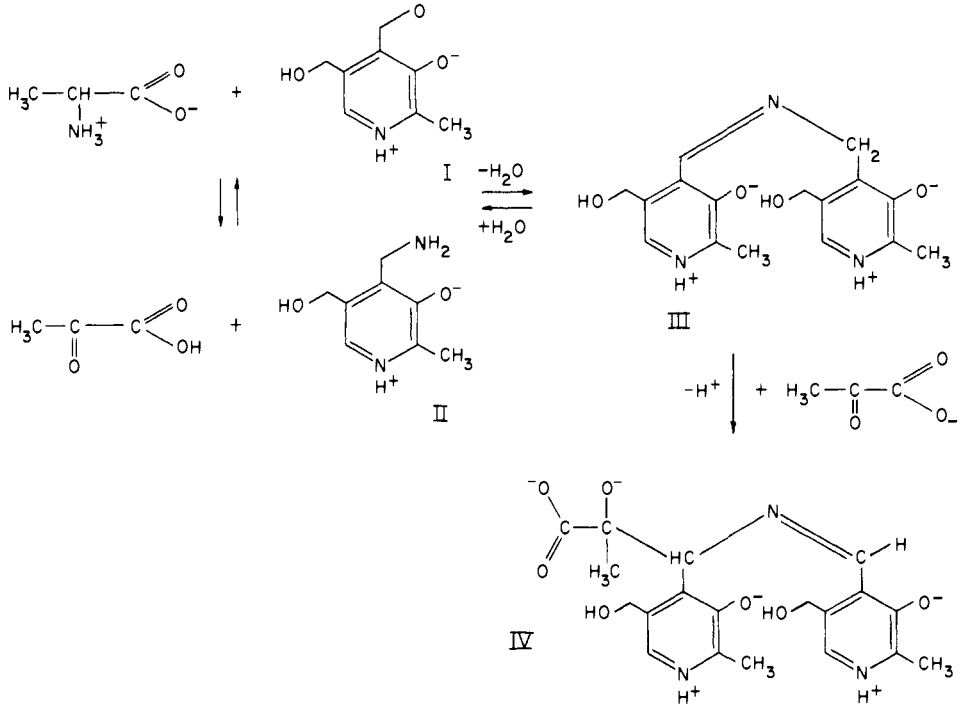

compounds, as determined from computer-optimized least-squares fits to the experimental data, are included in Table VII. The observed quadrupole interaction, ΔE_Q, and isomer shift, δ, values are those expected for high-spin iron(III) complexes.[31,33] The first two compounds listed in Table VII contain six-coordinate iron(III), whereas the last three all contain five-coordinated iron(III). $Fe(Sane)_2Cl$ is a monomer, while the remaining compounds are all dimers (see Table IV). As might be expected, the five-coordinate compounds have larger quadrupole splittings because of the larger electric field gradient at the nucleus resulting from the open coordination site. There seems to be no obvious trend in the isomer shift with coordination number or the nature of the coordinated atoms. The rather large increase in the percent effect with decreasing temperature (see Figure 3) is indicative of a low Debye temperature for this material and is typical of all the compounds studied. At this time we have no explanation for the rather high line widths, Γ_i, found in $\{[Fe(N(PL)_2ala)]ClO_4\}_2 \cdot 2.6H_2O$. The observed asymmetry in the relative area and intensity of the two quadrupole split lines, which is especially pronounced at room temperature, is typical of complexes of this type.[23,30,31] Although this asymmetry could result from partial polycrystalline orientation in the absorber, this seems unlikely because the asymmetry tends to decrease with decreasing temperature. It seems more likely that this observed asymmetry could result from spin–spin relaxation effects.[34,35] We are currently studying the high- and low-temperature Mössbauer spectra of several of these dimers in order to better understand this asymmetry.

Reaction Pathway. Because of the unusual nature of the ligand, IV, found in $\{[Fe(N(PL)_2ala)]ClO_4\}_2 \cdot 2.6H_2O$ it seems necessary to discuss the reaction sequence which has led to this previously unreported compound.[10] It has been known for some time that divalent and trivalent metal ions will catalyze the transamination reaction through the formation of an intermediate Schiff-base complex between pyridoxal and an amino acid, in this case alanine.[2-5] Hence, it is apparent that the presence of trivalent iron, resulting from air oxidation of the divalent iron reactant, results in the formation of an equilibrium (Scheme I) between pyridoxal (I) and alanine, and pyridoxamine (II) and pyruvic acid. After the establishment of this equilibrium, it is possible for the resulting pyridoxamine to undergo a Schiff-base condensation with pyridoxal to form the Schiff base III.[8] This Schiff base has been reported earlier[9] and was found to form chelation complexes with trivalent aluminum and divalent copper. In these monomeric complexes, coordination apparently occurs through the two phenoxy groups and the imine nitrogen. Once III is formed it may undergo a rapid reversible α-proton to γ-proton shift across the imino group. It is also possible for the imino group in III to undertake nucleophilic attack at the α-keto carbon atom in the pyruvic acid present in the solution. This results in the formation of $N(PL)_2ala$ (IV),

(33) Greenwood, N. N.; Gibb, T. C. "Mössbauer Spectroscopy"; Chapman and Hall: London, 1971.

(34) Blume, M. *Phys. Rev. Lett.* **1965**, *14*, 96.

(35) Wickman, H. H.; Klein, M. P.; Shirley, D. A. *Phys. Rev.* **1966**, *152*, 345.

which then chelates across the two iron(III) ions as found in the structure shown in Figure 1.

Acknowledgments. It is a pleasure to acknowledge the helpful discussions which were held with Drs. J. A. Bertrand, M. P. O'Hara, and S. B. Hanna during the course of this work. The financial assistance of the National Science Foundation through Grants CHE 75-20417 and CHE 77-08325 is greatly appreciated.

Supplementary Material Available: Observed and calculated structure factors (15 pages). Ordering information is given on any current masthead page.

Stereoselective Synthesis and DNMR Study of Two 1,8,15,22-Tetraphenyl[1_4]metacyclophan-3,5,10,12,17,19,24,26-octols[1,2]

A. G. Sverker Högberg

Contribution from the Department of Organic Chemistry, Royal Institute of Technology, S-100 44 Stockholm, Sweden. *Received December 13, 1979*

Abstract: The acid-catalyzed condensation of resorcinol with benzaldehyde initially gives a mixture of two stereoisomeric 1,8,15,22-tetraphenyl[1_4]metacyclophan-3,5,10,12,17,19,24,26-octols (**1a** and **1b**). The kinetically favored isomer **1a** is converted into the thermodynamically more stable one (**1b**), which subsequently is obtained in high yield (>80%) after longer reaction times. The configurations and conformations of the two isomers were investigated using molecular model and symmetry considerations combined with dynamic NMR measurements on the corresponding octabutyrates (**2a** and **2b**) and on the octabutyrates of the resorcinol–*p*-bromobenzaldehyde condensation products (**4a** and **4b**). The **a** isomers possess a chair-like conformation with the phenyl groups, in pairs, in axial positions on each side of the plane of the macrocyclic ring (C_{2h} symmetry). The **b** isomers possess a boat-like conformation with all four phenyl groups in the axial positions below the plane of the macrocyclic ring (C_{2v} symmetry). The **b** isomers can undergo pseudorotation [$\Delta G^{\ddagger}_{378K}$ = 79.5 ± 0.4 kJ mol^{-1} (19.0 ± 0.1 kcal mol^{-1}) (**4b**)]. The $\Delta G^{\ddagger}_{258K}$ values for the independent free rotation of *p*-bromophenyl groups in the octabutyrates **4a** and **4b** were 49.2 ± 0.4 and 54.0 ± 0.4 kJ mol^{-1} (11.8 ± 0.1 and 12.9 ± 0.1 kcal mol^{-1}), respectively. The calculations of the anisotropic effects of the aromatic rings in the macrocycles, based on the Bovey–Johnson equation, were helpful in ruling out one of the tentative stereostructures. The stereoselectivity of the reactions is attributed to a combination of three factors: the nonbonded intramolecular steric interactions in the triphenylmethane units, the reversibility of the cyclooligomerization, and the solubility differences of the two macrocyclic products.

The acid-catalyzed condensation of a phenol and an aldehyde generally results in a complex, amorphous mixture of products often possessing very high molecular weights. At the same time it has long been known that some phenols, like resorcinol, react with certain aldehydes, like benzaldehyde[3] and salicylaldehyde,[4] to give crystalline products. The structures of these phenolic compounds, which possess high melting points and fairly low solubilities in most organic solvents, were unknown for a long time.

Some 40 years ago Niederl and Vogel studied the reaction of resorcinol with a few aliphatic aldehydes.[5] In each case they obtained a single product for which they proposed the general structure I (R = alkyl; R′ = H). In view of the large number of steric and structural isomers possible, the isolation of a single macrocyclic condensation product is intriguing and tempted us to reinvestigate these condensation reactions.

In a preliminary communication we reported that the acid-catalyzed condensation of resorcinol and benzaldehyde gave a mixture of two stereoisomeric macrocycles, possessing the same

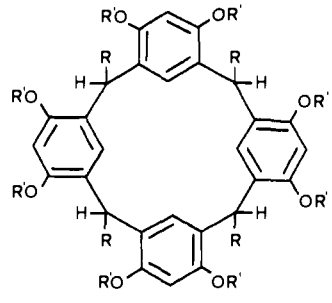

I

general [1_4]metacyclophane structure I (R = C_6H_5; R′ = H), in high yields.[6] The octabutyrate **4b** of one of the two resorcinol–*p*-bromobenzaldehyde condensation products was shown by X-ray crystallographic analysis to possess an all-axial and all-cis configuration of the phenyl groups with the macrocyclic ring in a boat-like conformation.[6-8]

In this paper we present the results of an extended study on the formation and degradation of the macrocycles in acid solution. The stereostructure of the second isomer **4a** was elucidated by correlation of the static and dynamic ^{1}H NMR data with molecular model and symmetry considerations and is in agreement

(1) (a) Cyclooligomeric Phenol–Aldehyde Condensation Products. 2. For part 1 see ref 6. (b) Taken in part from Högberg, A. G. S. Ph.D. Dissertation, Royal Institute of Technology, Stockholm, Sweden, 1977. (c) Part of this work was presented at the Euchem Conference on Ring Closure Reactions and Related Topics, Castel Gandolfo, Italy, Aug 29, 1978.

(2) Systematic names: **1a**, *r*-2,*c*-8,*t*-14,*t*-20-tetraphenylpentacyclo[19.3.1.1^{3,7}.1^{9,13}.1^{15,19}]octacosa-1(25),3,5,7(28),9,11,13(27),15,17,19(26),21,23-dodecaen-4,6,10,12,16,18,22,24-octol; **1b**, *r*-2,*c*-8,*c*-14,*c*-20-tetraphenylpentacyclo[19.3.1.1^{3,7}.1^{9,13}.1^{15,19}]octacosa-1(25),3,5,7(28),9,11,13(27),15,17,19(26),21,23-dodecaen-4,6,10,12,16,18,22,24-octol.

(3) (a) Baeyer, A. *Ber.* **1872**, *5*, 25. (b) Michael, A. *Am. Chem. J.* **1883**, *5*, 338. (c) Michel, A.; Ryder, J. P. *Ber.* **1886**, *19*, 1388. (d) Liebermann, C.; Lindenbaum, S.; Glawe, A. *Ibid.* **1904**, *37*, 1171. (e) Fabre, R. *Ann. Chim. (Paris)* **1922**, *18*, 82. (f) Mertens, E.; Fonteyn, M. *Bull. Soc. Chim. Belg.* **1936**, *45*, 186.

(4) Liebermann, C.; Lindenbaum, S. *Ber.* **1904**, *37*, 2728.

(5) Niederl, J. B.; Vogel, H. J. *J. Am. Chem. Soc.* **1940**, *62*, 2512.

(6) Erdtman, H.; Högberg, S.; Abrahamsson, S.; Nilsson, B. *Tetrahedron Lett.* **1968**, 1679.

(7) Nilsson, B. *Acta Chem. Scand.* **1968**, *22*, 732.

(8) An attempted X-ray analysis of the second octabutyrate isomer was unsuccessful because the inherent molecular symmetry caused a systematic absence of reflections which led to ambiguities in the crystal space group determination (Bo Nilsson, personal communication, 1969). Assuming the nonstandard space group $P2_1/n$, Palmer et al.[9] have, however, been successful with the corresponding octaacetate.

0002-7863/80/1502-6046$01.00/0 © 1980 American Chemical Society